TISSUE ENGINEERING: Part A
Volume 21, Numbers 1 and 2, 2015

DOI: 10.1089/ten.tea.2014.0151

Periodontal Cell Implantation Contributes to the Regeneration of the Periodontium in an Indirect Way

Na Yu, DDS, PhD,[1] Antonius L.J.J. Bronckers, PhD,[2] Daniel A.W. Oortgiesen, DDS, PhD,[1] Xiangzhen Yan, DDS,[1] John A. Jansen, DDS, PhD,[1] Fang Yang, PhD,[1] and X. Frank Walboomers, PhD[1]

Periodontitis is the most common human infectious disease. Regeneration of bone and soft tissue defects after periodontitis remains challenging, although the transplantation of periodontal ligament (PDL) cells seems a liable strategy. However, little is known about the function of PDL cells after transplantation. In the current study, a combination of *in vitro* coculture systems and *in vivo* immunohistochemistry (IHC) was used to investigate the role of PDL cells in the regenerative process. First, a coculture method was used, in which mesenchymal cells (representing the host tissue) were brought into direct contact with PDL cells (representing the transplanted cell population). It was found that PDL cells significantly increased mineralized matrix formation and osteocalcin expression, whereas control cells did not. Similar results were obtained when a noncontact coculture system was applied separating PDL and mesenchymal cells. In an *in vivo* rat model, regeneration of alveolar bone and ligament was seen after PDL cell transplantation. Implanted PDL cells were found clustered along the newly formed tissues. IHC showed enhanced osteopontin expression and gap junction staining in areas neighboring implanted PDL cells. In conclusion, PDL cells enhance periodontal regeneration through a trophic factor stimulating the osteogenic activity of the surrounding host cells.

Introduction

Periodontitis is the most common infectious disease in humans and a leading cause of tooth loss. Periodontitis results in the damage of tooth supporting tissues, including alveolar bone, periodontal ligament (PDL), tooth cementum, and gingiva. Current conventional clinical treatments to eradicate the clinical symptoms of periodontitis hardly result in regeneration of lost tissues. To achieve periodontal regeneration is a challenging task, since multiple tissues need to be formed in a spatial and temporal order. Due to the improved understanding of wound healing and advances in biology and biomaterial science, current research in tissue engineering can offer a promising approach to achieve this aim.[1] This concept aims to create or regenerate functional tissues through the use of an appropriate combination of three fundamental tools, namely, signaling molecules, engineering scaffolds, and cells, which together are also known as the tissue engineering triad.[2] Cells are of no doubt central to the effectiveness of tissue engineering strategy. PDL cells have been reported to possess the potential to restore the hard and soft periodontal tissues into their original architecture in many studies, using surgically created defects in animal models.[3,4] For instance, previously, we reported a rat model, in which transplantation of PDL cells onto a gelatin matrix led to functional regeneration of alveolar bone and morphologically correct organized ligament.[4]

Despite such success in preclinical models, little is known about how the implanted PDL cells can actually contribute to regeneration. Better understanding of the events involved in the cell-based regeneration process is central to improve clinical potential. From previous transplantation studies with mesenchymal cells, it is known that implanted cells can contribute to tissue regeneration by two possible routes; that is, form tissue by themselves (direct contribution) or by secreting cytokines/growth factors inducing host cells to form new tissues (indirect contribution).[5] Also, in the periodontal regeneration process, both options could be accurate. The microenvironment of periodontal defect is filled not only with the implanted cells but also surrounded by PDL cells and mesenchymal cells from the alveolar bone or peripheral blood of the host. Since the PDL cell population contains fibroblasts, osteoblasts, cementoblasts, and stem cells, lost tissues might be restored as a result of direct regeneration. Alternatively, the PDL cells could also actively interact with the surrounding host cells and promote the endogenous healing ability of host tissues, in a mechanism of indirect regeneration. In the current study, we investigated the

[1]Department of Biomaterials, Radboud University Nijmegen Medical Center, Nijmegen, The Netherlands.
[2]Department of Oral Cell Biology, Academic Center for Dentistry (ACTA), Research Institute MOVE, Universiteit van Amsterdam and Vrije Universiteit, Amsterdam, The Netherlands.

cell interaction by *in vitro* coculture systems and further assessed the correlation and contribution of transplanted PDL cells to tissue regeneration in a rat maxillary periodontal defect model.

Materials and Methods

Isolation of PDL cells, gingival fibroblasts, and bone marrow cells

All procedures were performed according to the ethics committee approval (Radboud University Nijmegen Medical Centre RU-DEC 2010-028). For the *in vitro* study, bone marrow cells (BM) were retrieved from Wistar rats, as described before.[6] Primary PDL cells and gingival fibroblasts (GF) were retrieved from green fluorescent protein (GFP) transgenic SD rats (Japan SLC, Inc., Shizuoka, Japan), as described previously.[4] Briefly, PDL was scraped from the middle third of the extracted incisor roots, avoiding contamination of epithelial or pulpal cells. The freed portions of the PDL were minced and transferred to a T-25 flask, filled with 4 mL of culture medium. Thereafter, cells were expanded and maintained in the alpha minimal essential medium (αMEM; Gibco, Grand Island, NE) supplemented with 10% fetal bovine serum (FBS; Sigma, St. Louis, MO), 100 U/mL penicillin, and 100 μg/mL streptomycin (Gibco). Upon subconfluency, cells were released and subcultured. The cells were counted and subsequently frozen until further use. PDL cells were expanded and their calcification ability was confirmed by alkaline phosphatase (ALP) activity, as described previously.[7] For GF, a similar primary culture process was applied to the palatal gingiva tissues of the same donor rat according to Bruckmann *et al.*,[8] to be used as a negative control cell type for all experiments. GF were confirmed to be negative for the ALP activity. Cells of passage 4 were used from both cell types for the *in vitro* assays and *in vivo* implantation.

In vitro *coculture*

To investigate the effects of cell implantation *in vitro*, we studied the effect of PDL and GF cells onto undifferentiated mesenchymal cells derived from rat bone marrow. Two coculture systems were used. First, direct contact coculture was performed by seeding $1\times10^4/cm^2$ GF or PDL cells (representing the implanted cell population), together with BM (representing the mesenchymal cells of the host) at a 1:1 ratio. Monocultures of BM, GF, or PDL were used as controls. In this system, paracrine effects as well as direct cell–cell contact are possible. Second, a noncontact coculture was established by seeding BM in the bottom of a transwell dish at $1\times10^4/cm^2$, that is, 2×10^4 cells in total. Thereafter, the same amount of BM, GF, or PDL cells was added to the top well inserts (pore size 0.4 μm; Greiner Bio-One, Frickenhausen, Germany). In this system, only paracrine factors could affect the performance of BM cells.

In both systems, cells were cultured for 14 days in the osteogenic medium containing 10% FBS, 10 mM sodium β-glycerophosphate, 10^{-8} M dexamethasone, 50 μg/mL ascorbic acid, 100 U/mL penicillin, and 100 μg/mL streptomycin (all from Gibco).

Cell distribution in vitro

After 3 and 14 days of direct contact coculture, cells were fixed in 3% paraformaldehyde (Sigma) and 0.02% glutaraldehyde (Acros, Geel, Belgium), permeabilized in 0.5% Triton100 (Koch, Colnbrook, United Kingdom), and subsequently blocked with 5% bovine serum albumin (Sigma). Actin was fluorescently stained with Alexa fluor 568-conjugated phalloidin (1:50; Molecular Probes, Invitrogen Corp., Paisley, United Kingdom), and cell nuclei were stained with DAPI (1:2500; Molecular Probes, Eugene, OR). In this way, GF/PDL cells were distinguished from BM cells by the GFP (green) signal together with actin (red) staining, whereas BM cells were stained in red only. Specimens were examined using an automated microscope (Imager Z1; Zeiss, Heidelberg, Germany).

Mineralized matrix deposition

Mineralized matrix formation was evaluated by assessing the Ca^{2+} content. For indirect contact culture samples, only the calcium content in the bottom BM cell layer was assessed. In brief, samples were rinsed and supplemented with 0.5 mL acetic acid (0.5 N) overnight. A volume of 10 μL samples was incubated with 300 μL of ortho-cresolphtalein complexone (OCPC; Sigma) working solution. Values were calculated comparing to a standard curve of $CaCl_2$ ranging from 1 to 100 μg/mL.

In vitro *gene expression assays*

The mRNA of cells at day 14 of culture was extracted using the GenElute™ Mammalian Total RNA Miniprepkit (Sigma). After obtaining the mRNA, a first-strand reverse transcriptase PCR was performed using the Superscript™ III First-strand Synthesis System for RT-PCR (Invitrogen). The cDNA was then amplified, and specific gene expression using rat-specific primers (Table 1) was quantified in a real-time PCR apparatus (Bio-rad CFX96; Bio-Rad, Hercules, CA). The expression of the tested osteogenic genes was

Table 1. Overview of the Sequences of Used Primers

Gene	*Forward (5′→3′)*	*Reverse (5′→3′)*	*NCBI reference sequence*
Col I	GAGCGATTACTACTGGATTGACCC	CAAGGAATGGCAGGCGAGAT	NM 053356
ALP	GGGACTGGTACTCGGATAACGA	CTGATATGCGATGTCCTTGCA	NM_007431
OCN	CGGCCCTGAGTCTGACAAA	GCCGGAGTCTGTTCACTACCTT	X04142
BSP	TCCTCCTCTGAAACGGTTTCC	GGAACTATCGCCGTCTCCATT	NM 008318
β-Actin	TTCAACACCCCAGCCATGT	TGTGGTACGACCAGAGGCATAC	NM 031144

ALP, alkaline phosphatase; BSP, bone sialoprotein; OCN, osteocalcin.

calculated using the $2^{-\Delta\Delta Ct}$ method versus the housekeeping gene β-actin and relative to the BM group.

In vivo *study*

Samples for the *in vivo* immunohistochemistry (IHC) were obtained from a previously described animal study for PDL cell transplantation, which showed a significant restoration of alveolar bone height as well as the formation of functionally oriented ligament tissue.[4] In brief, gelatin sponges (Spongostan®; Ferrosan Medical Devices, Soeborg, Denmark) of 2×2×2 mm were used as the cell carrier. The PDL and GF cells were loaded onto the scaffolds (1.0×10^6 cells/scaffold) 1 day before implantation. Empty scaffolds were incubated in the same circumstances as the other cell groups. Subsequently, cell–scaffold constructs were kept and transferred in the cell culture medium until implantation. GFP fluorescent signals were detected to confirm that comparable amount of cells between the GF and PDL groups were transplanted, as previously described.[4] Twelve athymic nude rats (NIH Foxn1^{rnu}; Charles River, Sulzfeld, Germany) were used as the recipient animals for cell transplantation. Under general inhalation anesthesia, bilateral intrabony three-wall defects were created mesial of both maxillary first molars. Thereafter, three types of scaffolds were divided randomly over defects in all animals, that is, loaded with PDL cells, loaded with control GF cells, or empty scaffolds ($n=8$). After scaffold placement, flaps were repositioned and sutured. Six weeks after surgery, rats were sacrificed followed by 10% formalin cardiovascular perfusion. Complete maxillas were retrieved, fixed in buffered 10% formaldehyde (1 day), and decalcified in 4% EDTA at 4°C for 6 weeks. Thereafter, samples were dehydrated through graded ethanol, cleared with xylene, and embedded in paraffin. Serial sections (thickness 6 μm) were cut using a microtome (Leica RM2165, Nussloch, Germany) in a mesiodistal plane.

IHC and histomorphometry

For each specimen, hematoxylin and eosin staining was first performed to determine the location of the defect area and bone formation. Subsequently, one slide with three continuous tissue sections from the middle third of the surgical defect was used for the IHC. These tissue sections were used to correlate the implanted cells (GFP, 1:400, rabbit anti IgG fraction; Molecular Probes) and protein markers: osteocalcin (*OCN*, rabbit anti rat dentin *OCN*, a gift from W.T. Butler, Houston, TX; 1:10), bone sialoprotein (*BSP*, mouse anti rat *BSP*; Developmental Studies Hybridoma Bank [DSHB], IA, cat. no. WV1D1 9C5; 1:200), osteopontin (*OPN*, mouse anti rat *OPN*, DSHB, cat. no. MPIIIB 101, 1:400), and connexin 43 (*CN43*, rabbit anti connexin 43; affinity purified Abcam, cat. no. Ab11370, 1:200).

Specifically, from three consecutive tissue sections, the first was used as negative control, the second for anti-GFP staining, and the third for the osteoblast marker protein. Sections were deparaffinized, rehydrated, and rinsed in PBS. Antigens were retrieved with a citrate buffer (pH 6.0) at 95°C for 20 min (except for anti-CN43, EDTA was used as a retrieval buffer). Thereafter, endogenous peroxidase was blocked (Envision kit; DakoCytomation; Glostrup, Denmark); and sections were preincubated in 30% normal goat serum. Next, sections were incubated with primary antibodies overnight at 4°C within a humid atmosphere. Subsequently, sections were washed and incubated with second antibodies (goat anti-rabbit IgG conjugated with peroxidase polymer or goat anti-mouse IgG conjugated with peroxidase polymer; Envision). After washing, the peroxidase conjugates were visualized with the 3,3′ diaminobenzidine (DAB)

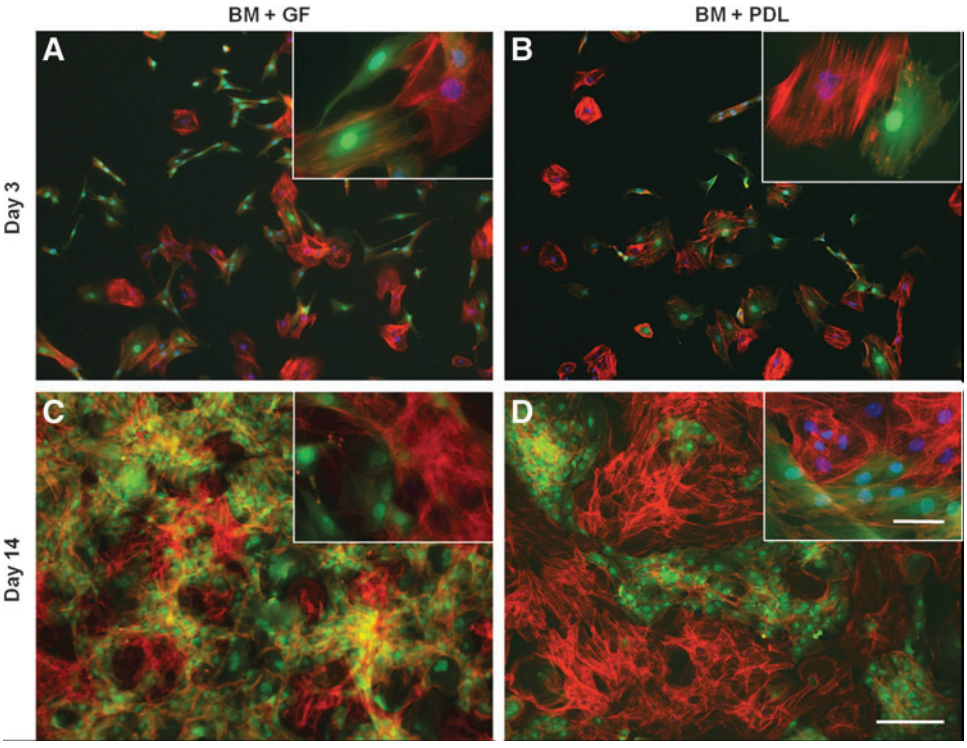

FIG. 1. Cell morphology in direct contact coculture: cells stained in red only are BM cells; cells in combined red and green/bright yellow are GF/PDL cells. **(A)** and **(C)** BM cocultured with GF after 3 and 14 days; **(B)** and **(D)** BM cocultured with PDL after 3 and 14 days. The insert images are higher magnification of each image. Scale bars = 200 and 50 μm for insert images. BM, bone marrow cells; GF, gingival fibroblasts; PDL, periodontal ligament.

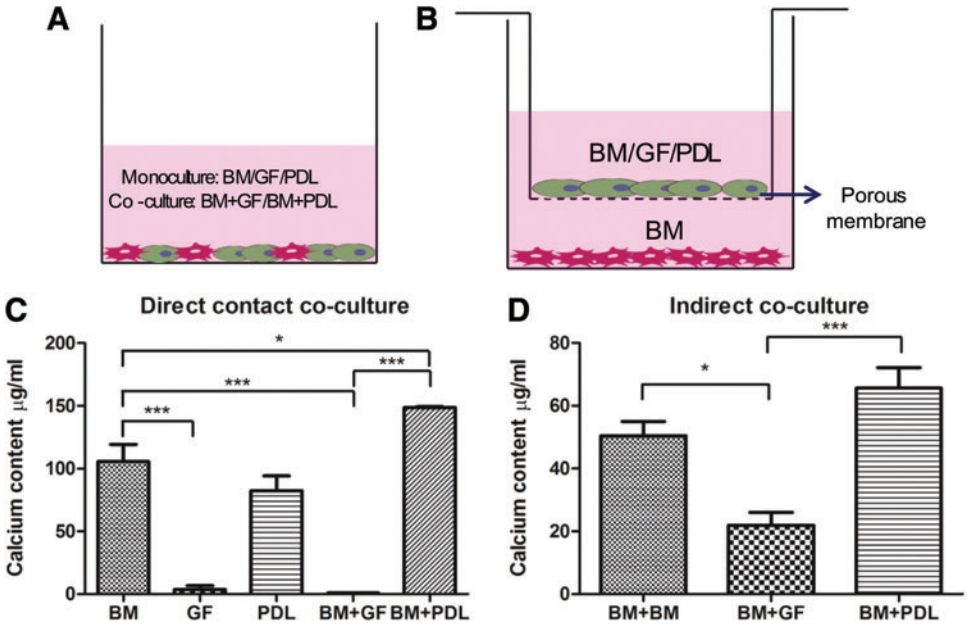

FIG. 2. Assays for *in vitro* coculture. **(A)** Direct contact coculture system; BM cells (red) were mixed with GF/PDL cells (green); monocultures of BM/GF/PDL were applied as controls. **(B)** Indirect coculture system; BM cells were cultured separately with BM/GF/PDL by a porous membrane. **(C, D)** Calcium content in direct and indirect cocultures upon 14 days of culture; values are given as the mean ± standard deviation (SD). $*p<0.05$, $**p<0.01$, $***p<0.001$ as compared with the BM group ($n=4$). Color images available online at www.liebertpub.com/tea

substrate (Envision), and nuclei were stained with hematoxylin. The area of GFP+stained cells was assessed by normalizing the DAB-stained areas toward the region of interest (ROI, defined as the distance between the surgical margins of hard tissue defect and the height of the original bone plate).

Statistical analysis

Samples were tested quadruplicate for each *in vitro* test. Means and standard deviations were calculated, and the statistical significance of differences between groups was examined using one-way analysis of variance (ANOVA) with Bonferroni's multiple comparison test (Instat version 3.05; GraphPad, Inc., San Diego, CA). Test results were considered statistically significant for probability values of $p<0.05$.

Results

Cell distribution in the coculture system

In the direct contact coculture setup, the distribution and morphology of the different cell types were assessed. After 3 days, both the PDL and GF control cells had attached and were mixed evenly through the BM cells. Due to the combined green/red signals, PDL and GF appeared as bright yellow and were spreading in a spindle-like shape. Stained in red only, BM showed a larger cell surface area and a spherical shape. After 14 days of culture, cells reached confluence. The GF cells stayed mixed with BM in an evenly dispersed manner. In sharp contrast, PDL cells always were growing in clusters meeting with BM at the circumference (Fig. 1).

Mineralized matrix deposition

Based on the two coculture systems, as shown in Figure 2A and B, the calcium content was assessed after 14 days of culture. In monocultures, a high formation of mineralized matrix was observed in BM cells, whereas GF cells did not mineralize. The Ca^{2+} content for PDL cells was intermediate. In the direct contact coculture, the BM+GF mixture showed a significant lower calcium amount than BM

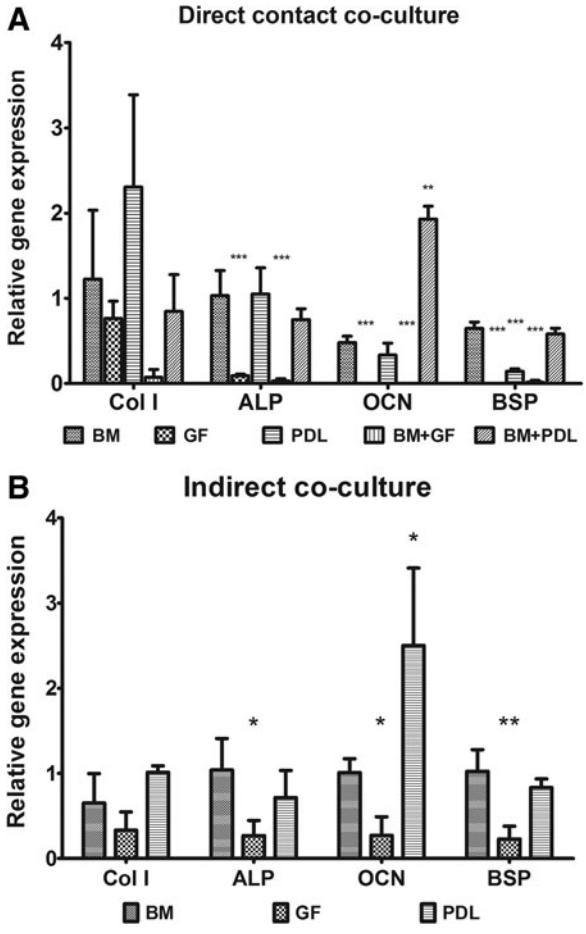

FIG. 3. Profiles of osteogenic genes expressed in the direct contact co-culture **(A)** and indirect co-culture **(B)** systems, as measured by RT-PCR; values are given as the mean ± SD. $*p<0.05$, $**p<0.01$, $***p<0.001$ as compared with the BM group ($n=4$).

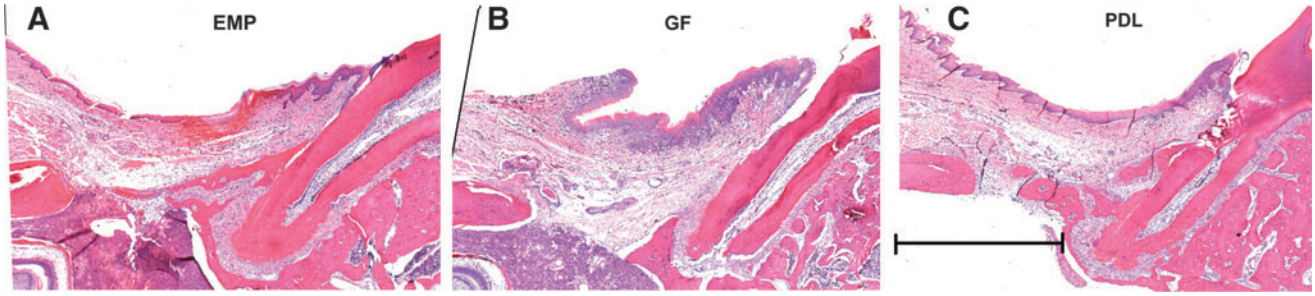

FIG. 4. Histological overview of different treatment groups: **(A)** empty scaffold group; **(B)** GF-loaded group; **(C)** PDL cell-loaded group. Scale bar = 2 mm.

monoculture. In contrast, the BM + PDL mixture significantly promoted matrix calcification compared to both BM and PDL monocultures (Fig. 2C). In the indirect coculture system, the Ca^{2+} deposition tests were applied to the BM cells in the bottom layer only, thus on values average to about half of those assessed in the direct coculture. Still, the indirect coculture always demonstrated the same trends among the three groups (Fig. 2D).

In vitro *gene expression*

The mRNA expression of osteogenic markers collagen I, ALP, OCN, and BSP is shown in Figure 3A and B. In monoculture, only the GF control cells did not show expression of OCN and BSP. The PDL cells always showed comparable levels of expression in all the tested genes compared with BM, except for BSP. Direct coculture of PDL and BM yielded an upregulation of OCN expression, while maintaining similar expression levels of Col I, ALP, and BSP compared with BM monoculture. In contrast, gene expression in the BM + GF coculture showed inhibition of all osteogenic marker genes. Again, in the noncontact coculture, the expression of all markers followed a similar trend as in the direct coculture, meaning the presence of PDL, without direct contact, still upregulated the OCN expression of BM. In contrast, the presence of GF downregulated the expression levels of ALP, OCN, and BSP in the BM cells.

General observation of in vivo *histology*

In the histological sections of the *in vivo* study, the defect areas could be distinguished in all samples (Fig. 4A–C) by the interruption of hard tissue between the mesial root surface of the first molar and the original margins of the bone plate. Within the defect, the gelatin scaffolds could not be identified in the defect area anymore and apparently had degraded.

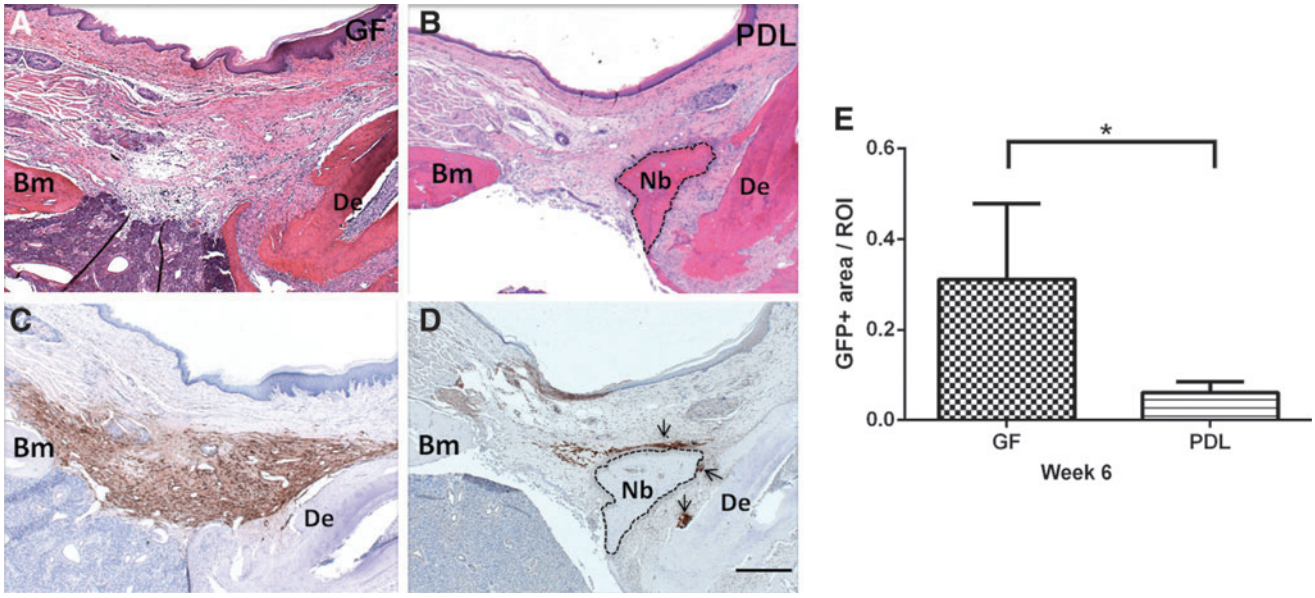

FIG. 5. HE staining and corresponding anti-GFP staining: **(A)** HE staining of GF cell implanted periodontal defect; **(B)** HE staining of PDL cell implanted periodontal defect; **(C)** GF cells were distributed extensively between the alveolar bone margin and dentin surface; **(D)** PDL cells were only located in the confined areas around the newly formed tissues; **(E)** histomorphometrical analysis of the positive stained area ratio of GF and PDL implanted cells in the defect regions. ROI is defined as the hard tissue defect from the surgical margins of cortical bone and root surface. Dotted close-ups indicate the areas of newly formed bone and arrows indicate positive GFP cells. Scale bar = 500 μm **(A, B)**; $*p < 0.05$. Bm, bone margin; De, dentin; Nb, newly formed bone; GFP, green fluorescent protein; HE, hematoxylin and eosin; ROI, region of interest.

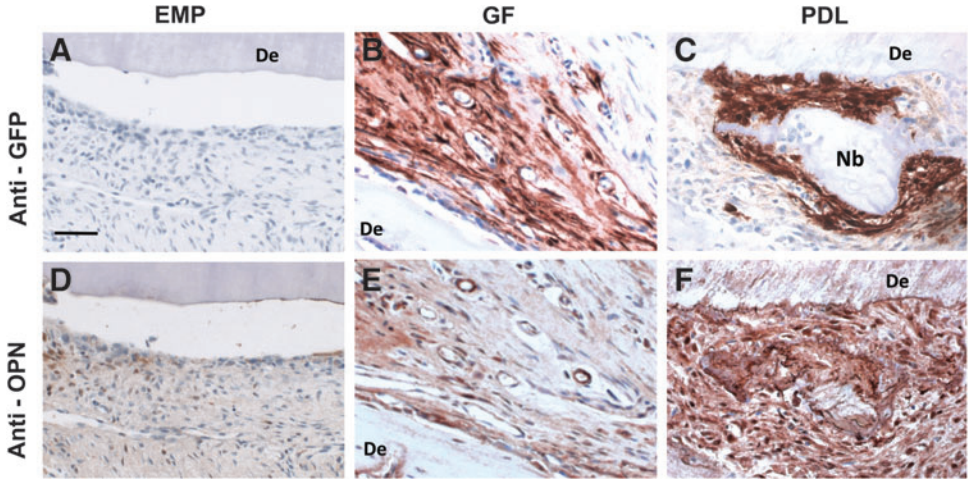

FIG. 6. Anti-*OPN* immunohistochemical staining: **(A)** higher magnification of anti-GFP staining shows no GFP signal in the empty scaffold group; **(B)** implanted GFP + GF cells were loosely connected with each other, **(C)** whereas PDL cells were closely in contact with surrounding cells. **(D–F)** Anti-OPN staining; more intense staining was shown in the PDL cell surrounding areas than GF surrounding areas and regions close to dentin in the empty scaffold group. Scale bar = 50 μm. De, dentin; Nb, newly formed bone; OPN, osteopontin.

In the group with empty (nonseeded) scaffolds, a new bone formation was found deriving from the apical area of the root area (Fig. 4A). In the GF-seeded group, less bone was seen in the defect areas, as compared to the empty scaffolds (Fig. 4B). In the PDL group, newly formed bone was observed at the mesial/apical defect edges and was more pronounced compared with the other groups (Fig. 4C). Besides bone being present at the defect margin areas, new bone could also be detected as separate islands, that is, without apparent direct contact with the defect edges.

IHC staining

No GFP signal could be detected in the empty control group without cells and with scaffold only. In the group implanted with GF cells, GFP + cells could be found in all samples (8/8). The GF cells were distributed extensively between the surgically created alveolar bone margin and the denuded dentin surface (Fig. 5A, C). In contrast, in the PDL group, the GFP + cells only appeared in four out of eight samples (4/8). The PDL cells were always located in the connective tissues, clustered in a highly concentrated manner, and closely surrounding the areas of the newly formed bone (Fig. 5B, D). Quantification corroborated that PDL cells were concentrated over a smaller area than GF cells at 6 weeks postimplantation (Fig. 5E). Higher magnification micrographs revealed that the GFP + GF cells were loosely connected in contrast to the GFP + PDL cells, which exhibited a very intimate cell–cell contact (Fig. 6A–C). Only occasionally separate GFP + PDL cells were found inside areas of newly formed bone.

Due to high nonspecific staining, anti-OCN and anti-BSP staining could not be used for comparison between the groups. Still, the location of GFP + cells could be compared with the anti-OPN staining. In all the samples with GFP + cells, a more intense expression of OPN was consistently seen in the tissue grafted with GFP + PDL cells compared with the GF cells (Fig. 6D–F). In the empty scaffold group, only minor and scattered OPN staining cells were observed, adjacent to the dentin surface. Subsequently, by comparing

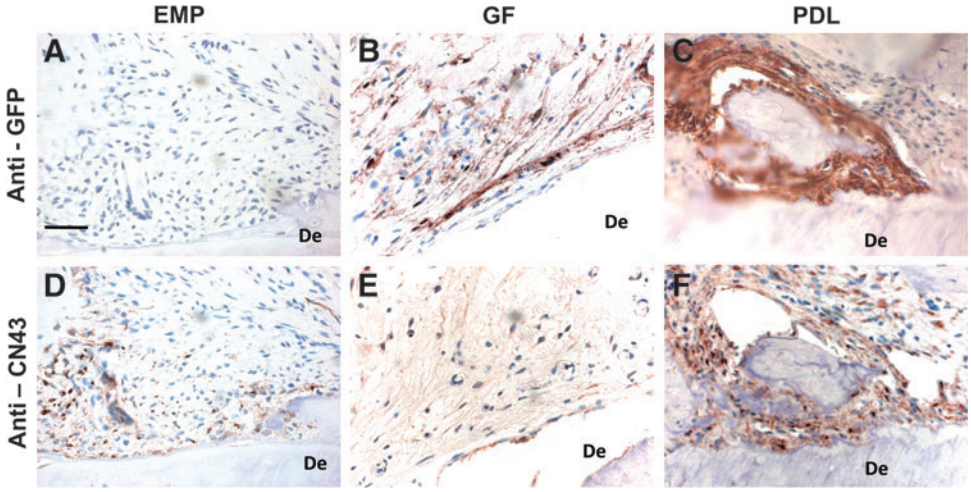

FIG. 7. Anti-*CN43* immunohistochemical staining: **(A–C)** indication of anti-GFP staining. **(D–F)** Anti-*CN43* staining shows more intense gap junction among and around the PDL cell area than GF cells and the empty scaffold region. Scale bar = 50 μm. De, dentin; CN43, connexin 43.

the location of GFP cells with anti-*CN43* staining, it was shown that the PDL cell areas gave an enhanced tissue expression of gap junctional protein, as compared to both the GF cells and empty scaffold group (Fig. 7A–F).

Discussion

The objective of this study was to elucidate whether implanted PDL cells can directly contribute to newly formed bone tissue during the periodontal regeneration or instead act as a source of growth factors and cytokine stimulating host cells. Both an *in vitro* coculture system and *in vivo* model were used. The results from this study support the concept that a paracrine effect of implanted PDL cells has evident influence on the local host cellular dynamics, and at least mainly in such a way that governs the regeneration process.

Regarding the *in vitro* setup, it is known that periodontal repair involves progenitor cells, capable of forming fibroblasts, osteoblasts, and cementoblasts.[9] In this context, we developed culture models, in which undifferentiated bone marrow mesenchymal stromal cells were selected to represent the host tissue. On the one hand, contact coculture was introduced to observe the effect on mineralization and gene expression. Changes in such data could reflect an influence of either soluble factors or direct cell–cell interactions. On the other hand, the indirect coculture system provided the possibility to investigate the cross talk between cell layers, by soluble mediators only. Since both systems provided very similar data, indeed it can be concluded that soluble factors are primarily involved. For the calcium measurement, it cannot be excluded that especially in the directly mixed cultures, there will be an altered growth rate of the different cells, thus influencing the number of mineralizing cells as well. Still, the mineral deposition data substantiate the hypothesis that PDL cells can orchestrate a cascade of bone formation, whereas GF cells clearly inhibited the osteogenic response in the recipient cells. In the gene assays, the fact that only *OCN* was upregulated may be due to the late stage of measurement at 14 days. This time point will be beyond the expression of ALP and other early markers. It is noted that transcription of osteogenic genes does not necessarily imply that the osteogenic factors are also being secreted by cells into the culture medium. A more comprehensive protein-level examination will help to unravel the exact factors and how they can take effect in the system.

Although both GF and PDL cells come from neighboring anatomical locations, their growth pattern in the mixed cocultures varied distinctly. The cluster-like manner in which PDL cells grew was in contrast with the scattered distribution of the GF cells. This phenomenon is strikingly consistent with the *in vivo* situation. Also *in vivo*, PDL cells after transplantation clustered along the defect area during the regeneration of a periodontal defect. In contrast, transplanted GF cells do not organize in nor contribute to periodontal regeneration.[4]

Regarding our *in vivo* experimental setup, GFP cells were introduced to investigate the role of implanted cells. Even in studies where the enhancement of periodontal regeneration has been quantified,[3,10] it is difficult to assess what portion of the newly formed tissue can be ascribed to implanted cells and what is due to other factors. Our results revealed that implanted PDL cells actually did hardly integrate into the newly formed tissues. This is consistent with recent findings with cell-labeling techniques, which demonstrated that only a small fraction of the cells remained in a defect after implantation in a calvarial defect model.[11] Our immunohistochemical data further revealed more intense *OPN* staining around PDL cells in the implanted areas compared with the GF. Furthermore, *CN43* gap junction staining indicated a more intense exchange of biological messenger molecules between implanted PDL cells and surrounding host cells. Since vertebrate gap junctions only allow transmembrane movement of small molecules,[12,13] such molecules may play a role to induce differentiation of precursor cells and activate osteoblasts to promote the regenerative process.[14]

Our *in vivo* results corroborate with other cell implantation studies in the current scientific literature. For example, Caplan and coworkers concluded that the main consequence of mesenchymal cell implantation is the functional (paracrine and autocrine) secretion of bioactive factors.[15] Such a trophic effect following cell implantation was found in many tissue regenerative processes, such as in brain defect regeneration,[16] a myocardial infarct model,[17] and meniscus regeneration.[15] Consistently, the MSC-mediated tissue restoration is suggested not to arise from the introduced MSCs, but rather by orchestration of the host cells.

In conclusion, our *in vitro* and *in vivo* findings demonstrated that transplanted PDL cells have the capacity to cluster and, thereafter, provide small molecular bioactive factors to reinforce the osteogenic activity of surrounding cells, which indirectly support the regeneration process.

Acknowledgments

We are grateful for the financial support from the Royal Netherlands Academy of Arts and Sciences (PSA) (08-PSA-M-02) and the China Scholarship Council (2008627114). The authors would like to thank Mrs. Monique Kersten-Niessen and Mr. Rene van Rheden for providing excellent technical help in gene expression assays and immunohistological staining.

Disclosure Statement

No competing financial interests exist.

References

1. Chen, F.M., and Jin, Y. Periodontal tissue engineering and regeneration: current approaches and expanding opportunities. Tissue Eng Part B Rev **16,** 219, 2010.
2. Langer, R., and Vacanti, J.P. Tissue engineering. Science **260,** 920, 1993.
3. Nakahara, T., Nakamura, T., Kobayashi, E., Kuremoto, K., Matsuno, T., Tabata, Y., *et al. In situ* tissue engineering of periodontal tissues by seeding with periodontal ligament-derived cells. Tissue Eng **10,** 537, 2004.
4. Yu, N., Oortgiesen, D.A., Bronckers, A.L., Yang, F., Walboomers, X.F., and Jansen, J.A. Enhanced periodontal tissue regeneration by periodontal cell implantation. J Clin Periodontol **40,** 698, 2013.
5. Caplan, A.I. Review: mesenchymal stem cells: cell-based reconstructive therapy in orthopedics. Tissue Eng **11,** 1198, 2005.
6. Maniatopoulos, C., Sodek, J., and Melcher, A.H. Bone formation *in vitro* by stromal cells obtained from bone marrow of young adult rats. Cell Tissue Res **254,** 317, 1988.
7. Oortgiesen, D.A., Yu, N., Bronckers, A.L., Yang, F., Walboomers, X.F., and Jansen, J.A. A three-dimensional

cell culture model to study the mechano-biological behavior in periodontal ligament regeneration. Tissue Eng Part C Methods **18,** 81, 2012.
8. Bruckmann, C., Walboomers, X.F., Matsuzaka, K., and Jansen, J.A. Periodontal ligament and gingival fibroblast adhesion to dentin-like textured surfaces. Biomaterials **26,** 339, 2005.
9. Melcher, A.H. On the repair potential of periodontal tissues. J Periodontol **47,** 256, 1976.
10. Flores, M.G., Yashiro, R., Washio, K., Yamato, M., Okano, T., and Ishikawa, I. Periodontal ligament cell sheet promotes periodontal regeneration in athymic rats. J Clin Periodontol **35,** 1066, 2008.
11. Tour, G., Wendel, M., Moll, G., and Tcacencu, I. Bone repair using periodontal ligament progenitor cell-seeded constructs. J Dent Res **91,** 789, 2012.
12. Hu, X., and Dahl, G. Exchange of conductance and gating properties between gap junction hemichannels. FEBS Lett **451,** 113, 1999.
13. Loewenstein, W.R. Permeability of membrane junctions. Ann N Y Acad Sci **137,** 441, 1966.
14. Ji, W., Wang, H., van den Beucken, J.J., Yang, F., Walboomers, X.F., Leeuwenburgh, S., *et al.* Local delivery of small and large biomolecules in craniomaxillofacial bone. Adv Drug Deliv Rev **64,** 1152, 2012.
15. Caplan, A.I., and Dennis, J.E. Mesenchymal stem cells as trophic mediators. J Cell Biochem **98,** 1076, 2006.
16. Chen, J., Li, Y., Katakowski, M., Chen, X., Wang, L., Lu, D., *et al.* Intravenous bone marrow stromal cell therapy reduces apoptosis and promotes endogenous cell proliferation after stroke in female rat. J Neurosci Res **73,** 778, 2003.
17. Tang, Y.L., Zhao, Q., Zhang, Y.C., Cheng, L., Liu, M., Shi, J., *et al.* Autologous mesenchymal stem cell transplantation induce VEGF and neovascularization in ischemic myocardium. Regul Pept **117,** 3, 2004.

Address correspondence to:
John A. Jansen, DDS, PhD
Department of Biomaterials
Radboud University Nijmegen Medical Centre 309 PB
PO Box 9101
Nijmegen 6500HB
The Netherlands

E-mail: j.jansen@dent.umcn.nl

Received: March 12, 2014
Accepted: June 25, 2014
Online Publication Date: July 30, 2014